

Determining the Full Halo Coronal Mass Ejection Characteristics

V.G. Fainshtein

Institute of Solar-Terrestrial Physics, Siberian Department,
Russian Academy of Sciences, Irkutsk, Russia

E-mail: vfain@iszf.irk.ru

Accepted: 21 December 2009

Abstract. Observing halo coronal mass ejections (HCMEs) in the coronagraph field of view allows one to only determine the apparent parameters in the plane of the sky. Recently, several methods have been proposed allowing one to find some true geometrical and kinematical parameters of HCMEs. In most cases, a simple cone model was used to describe the CME shape. Observations show that various modifications of the cone model ("ice cream models") are most appropriate for describing the shapes of individual CMEs. This paper uses the method of determining full HCME parameters proposed by the author earlier, for determining the parameters of 45 full HCMEs, with various modifications of their shapes. I show that the determined CME characteristics depend significantly on the chosen CME shape. I conclude that the absence of criteria for a preliminary evaluation of the CME shape is a major source of error in determining the true parameters of a full HCME with any of the known methods. I show that, regardless of the chosen CME form, the trajectory of practically all the HCMEs in question deviate from the radial direction towards the Sun-Earth axis at the initial stage of their movement, and their angular size, on average, significantly exceeds that of all the observable CMEs.

© 2010 BBSCS RN SWS. All rights reserved

Keywords: Sun, coronal mass ejection, prominence

Introduction

Full halo coronal mass ejections (HCMEs) are registered in the coronagraph field of view as regions of increased brightness, surrounding the occulting disk of the coronagraph in the plane of the sky and moving in all directions from the center of the solar disk. Howard et al, (1982) were the first to record a HCME [1]. A lot of full halos CMEs (HCMEs) were observed by the Large Angle and Spectrometric Coronagraph (LASCO) [2] on board the Solar and Heliospheric Observatory (SOHO) mission. Full HCMEs are considered to move from the Sun to the Earth if they are preceded by activity on the visible surface of the Sun: a flare etc. [3 - 6]. HCMEs play an important role in space weather [3, 6 - 8]. To time the arrival of such CMEs at the Earth and predict their geoeffective parameters at $R = 1$ AU it is necessary to determine the HCME geometrical and physical properties near the Sun.

Full HCME images in the coronagraph field of view may only be used to determine the apparent characteristics in the plane of the sky. Techniques for finding some geometric and kinematic parameters of full HCMEs in 3-D space were suggested and tested in [9-16]. Most methods assume a conical shape of CMEs [1, 17]. Observations of limb CMEs show, however, that the shape of each CME is best approximated by only one of the three modifications of the conical shape (ice cream cone models, [18]). This paper relies on the method in [16] to determine geometric and kinematic parameters of 45 full HCMEs for three possible modifications of their conical shape. I show that these parameters depend essentially on the selected CME shape modification.

Method of Determining the Full Halo CME Full Halo Parameters

Our analysis shows that there is a positive correlation between the angular size $\delta P-A$ of the eruptive prominence or post-eruptive limb arcade accompanying a CME observed in the LASCO C3 field of view, and the angular size 2α of the limb CME related to the prominence (arcade), Fig.1 [16, 19]. To find the CME width we used the SOHO/LASCO CME Catalog (http://cdaw.gsfc.nasa.gov/CME_list/) [2].

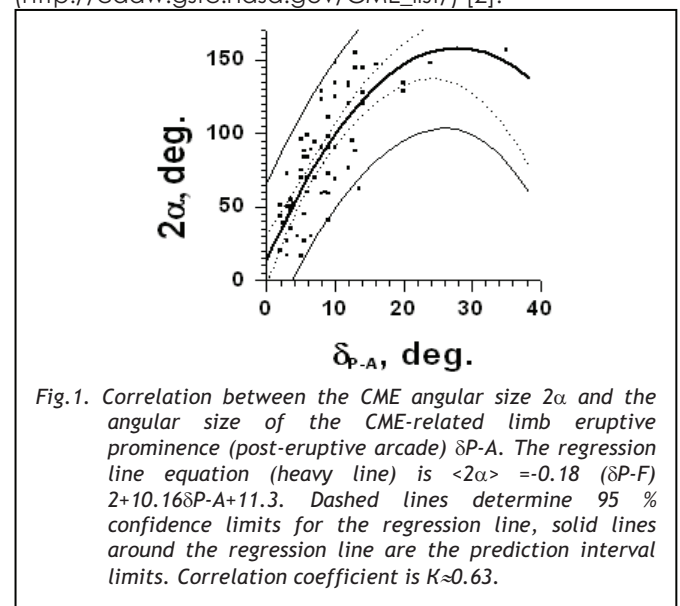


Fig.1. Correlation between the CME angular size 2α and the angular size of the CME-related limb eruptive prominence (post-eruptive arcade) $\delta P-A$. The regression line equation (heavy line) is $\langle 2\alpha \rangle = -0.18 (\delta P-A)^2 + 10.16\delta P-A + 11.3$. Dashed lines determine 95 % confidence limits for the regression line, solid lines around the regression line are the prediction interval limits. Correlation coefficient is $K \approx 0.63$.

This Catalog is improved and expanded in comparison with its first version [2] and described in the paper [7]. Besides, the paper [7] summarizes the statistical properties of CMEs such as a CME speed, width, acceleration, mass and kinetic energy. Eruptive prominence and/or post-eruptive limb arcade characteristics were determined from the extreme ultraviolet FeXII $\lambda 195\text{\AA}$ images of the Sun (SOHO/EIT). The scatter of points relative to the regression line in Fig.1 is due to several factors. One reflects the fact that it was not the true size of the prominence (arcade) that was determined but rather their projected size onto the plane of the sky. Preliminary analysis shows that a more exactly determined prominence (arcade) size, taking into account the orientation relative to the plane of the sky, reduces the dispersion of the data points. This paper does not use this result to correct the dependence in Fig.1 since the method for determining the true size of an eruptive structure is still under development.

Besides, the resulting reduction of the scatter in Fig.1 slightly affects the shape of the regression line to be used in the future. In accordance with [15], we will assume that the regression line in Fig.1 also connects the eruptive filament (EF) and/or the post-eruptive arcade (PEA) angular sizes on the visible disk of the Sun to the full HCME angular size associated with EF (PEA). Then, the angular size of such CMEs may be found using the regression line in Fig.1, in which $\delta P-A$ will mark now the eruptive filament (post-eruptive arcade) angular size on the visible disk of the Sun.

The other parameters of the full HCMEs were determined using the relations between the halo CME characteristics obtained for the three modifications of the CME cone model, Fig.2. For these models, we will use the following designations in this paper: cone-sphere (CS) model – Fig.2 (A), cone-semi-sphere (CSS) model – Fig.2 (B), and cone-sphere of big radius (CSBR) model – Fig.2 (C). This paper employees a limiting case of such a model – a conic model in which a model CME will consist only of a cone - as a CSBR model. These models differ in the ratio of the radius R_S of the spherical part the cone adjoins to the cone base radius R_C . The apex of the cone in Fig.2 is at the Sun center. Later, we plan to modify these models, resulting in the cone base becoming an ellipse, and the cone itself adjoining ellipsoids.

Fig.2 (A1-C1) shows sections of HCMEs in a plane passing through the axis of a model CME in three-dimensional space and through the Sun-Earth axis (axis X). The plane crosses the plane of the sky along the Y axis. Fig.2 (A2-C2) shows model HCME projections onto the plane of the sky. The Y axis is assumed in this paper to coincide with the direction in which the projection of a real HCME is displaced in the plane of the sky relative to the occulting disk center. In reality, this direction may differ from the Y axis direction within several degrees. This paper does not take this difference into account.

Fig.2 may be used to obtain expressions relating the full angular HCME size to its other parameters. To illustrate this, let us provide some formulas for the CS (equations (1)-(4)) and CSBR (equations (5)-(8)) models:

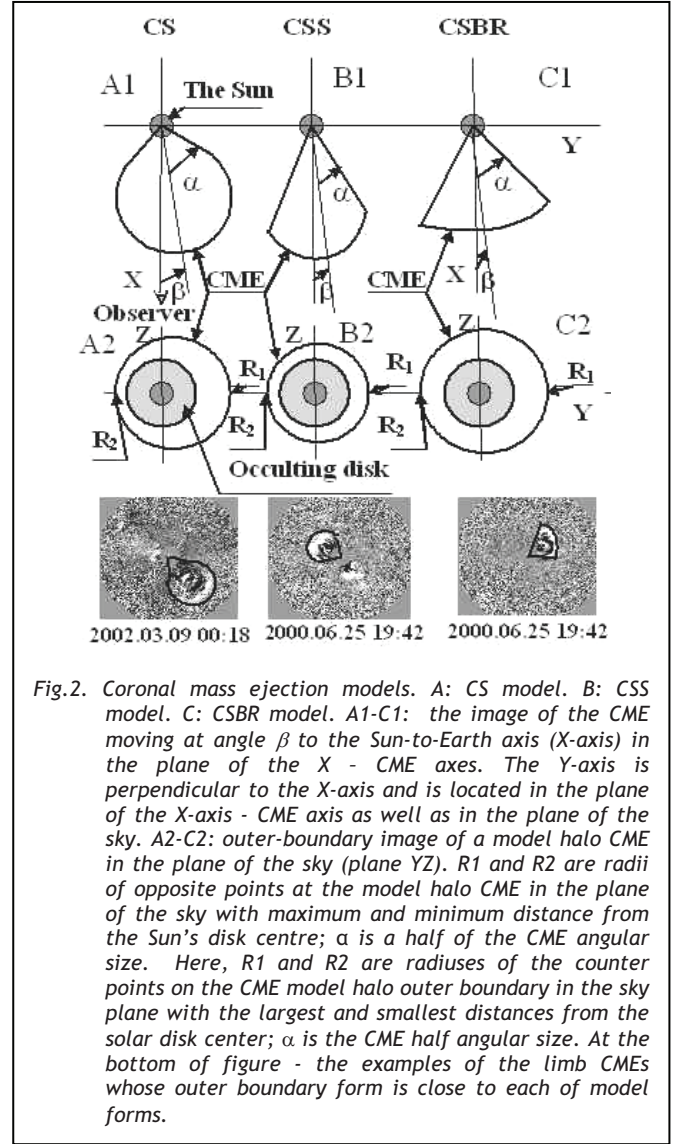


Fig.2. Coronal mass ejection models. A: CS model. B: CSS model. C: CSBR model. A1-C1: the image of the CME moving at angle β to the Sun-to-Earth axis (X-axis) in the plane of the X - CME axes. The Y-axis is perpendicular to the X-axis and is located in the plane of the X-axis - CME axis as well as in the plane of the sky. A2-C2: outer-boundary image of a model halo CME in the plane of the sky (plane YZ). R1 and R2 are radii of opposite points at the model halo CME in the plane of the sky with maximum and minimum distance from the Sun's disk center; α is a half of the CME angular size. Here, R1 and R2 are radiuses of the counter points on the CME model halo outer boundary in the sky plane with the largest and smallest distances from the solar disk center; α is the CME half angular size. At the bottom of figure - the examples of the limb CMEs whose outer boundary form is close to each of model forms.

$$\sin(\beta) = \frac{R - R_2}{R_1 + R_2} \sin(\alpha) \quad (1)$$

$$R_F = \left[\frac{R_1 + R_2}{2} \right] \frac{1 + \sin(\alpha)}{\sin(\alpha)} \quad (2)$$

$$V_F = V_1 \left[\frac{1 + \sin(\alpha)}{\sin(\beta) + \sin(\alpha)} \right] \quad (3)$$

$$V_{FE} = V_1 \left[\frac{\cos(\beta) + \sqrt{\sin^2(\alpha) - \sin^2(\beta)}}{\sin(\alpha) + \sin(\beta)} \right] \quad (4)$$

$$\text{tg}(\beta) = \frac{R_1 - R_2}{R_1 + R_2} \text{tg}(\alpha) \quad (5)$$

$$R_F = R_1 \frac{\cos(\alpha)}{\sin(\alpha + \beta)} \quad (6)$$

$$V_F = V_1 \frac{\cos(\alpha)}{\sin(\alpha + \beta)} \quad (7)$$

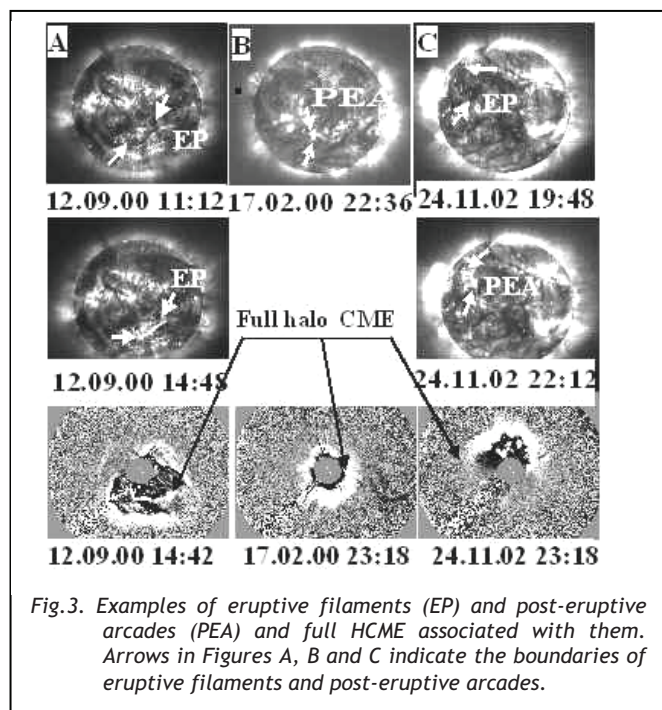
$$V_{FE} = V_1 \frac{\cos(\alpha)}{\sin(\alpha + \beta) \cos(\beta)} \quad (8)$$

Here, β is the angle between the HCME axis and the Sun-to-Earth axis, RF is the CME halo front radius on CME axis, V1 is the velocity of a point with radius R1, R1 is the largest, and R2 the smallest positions of the HCME image boundary visible in the sky plane, VF is the front velocity along the CME axis, VFE is the CME front velocity along the Sun-to-Earth axis. None of the parameters of the problem were supposed to be time-varying, for all the models under consideration.

Thus, the algorithm for determining the HCME parameters at a fixed instant of time consists of three steps: using the regression line in Fig.1 to find the HCME 2α angular size; using the CME halo images (LASCO C3) in the sky plane (see Fig.2) to determine the CME R1, R2 parameters; the β , RF, VF and VFE are found by means of equations (1) - (8) and similar formulas for other types of the CME conic models.

Determining the Observed Full Halo CME Characteristics

To test the method for determining the characteristics of full HCMEs we selected 45 coronal mass ejections associated with the eruption of a filament (EF) and/or with a post-eruptive arcade (PEA) using the SOHO/LASCO CME Catalog (http://cdaw.gsfc.nasa.gov/CME_list/) [2]. We also used for the analysis HCME parameters and its sources the special catalog of halo CMEs [6] (the URL of this Catalog is: http://cdaw.gsfc.nasa.gov/CME_list/HALO/halo.html).



The Catalog [6] contains both the information on properties of the halo CMEs, and data on characteristics connected with the halo CMEs flares (heliographic coordinates, the soft X-ray flare importance, and flare onset time). Moreover, the space speeds of HCME have been calculated using a CME cone model. EF and PEA characteristics were determined from SOHO's extreme ultraviolet imaging telescope (EIT) FeXII $\lambda 195\text{\AA}$ images. Figure 3 shows examples of the full halo CMEs under analysis and relevant EFs or PEAs. The arcade angular size $\delta P-A$ was determined between the arcade boundaries shown by arrows in Fig.3. The EF angular sizes ($\delta P-A$) were found as the angular distances between the "legs" of the eruptive filament at the initial stage of their eruption. R1 and R2 were determined along the main axis of the full HCME quasi-elliptic images based on LASCO C3 data at the instants of time when $R1 \approx (8-25) R0$, since at these distances the limb CME angular size changes only slightly: $2\alpha = \text{const.}$ [20].

To analyze the results, we also determined the angular position $\beta P-A$ of the EF and/or EPA center (within the heliocentric coordinate system). We used the linear fit velocity from the "SOHO/LASCO CME catalog" as V1.

Results

(i) Table 1 presents the averaged characteristics of the full halo CMEs under consideration obtained for the three CME cone models. One can see that the CME parameters found using various models differ distinctly. These differences should be considered significant if one applies, e. g., the results to determining the halo CME Sun-to-Earth transit time. Therefore, one has to additionally justify the use of a particular model in each specific case. The author believes this problem will be solved using STEREO data. Note that recently, based on expansion and radial speeds, Gopalswamy et al. (2009) [21] showed that the full ice cream cone (i.e. the CSS model of CME in our paper) best represents real CMEs. This was confirmed by Michalek et al. (2009) [22].

(ii) For all the halo CME models under consideration, the β -angle, characterizing the CME direction, differs significantly from the angular position $\beta P-A$ of the eruptive filament (of the post-eruptive arcade) related to the CME. For the overwhelming majority of CMEs under consideration we have $\beta < \beta P-A$. The author believes that the halo CME trajectory deviation from the radial direction towards the Sun-to-Earth axis is the most probable explanation of this inequality. Examples of the "limb" CME trajectory deviation from the radial direction can be found in literature ([5]).

TABLE 1
Comparison between the full halo CME parameters as determined using the three CME models; the angular brackets indicate mean values

Model\Parameter	$\langle\beta\rangle$, deg.	Min β , deg.	Max β , deg.	$\langle RF/R0 \rangle$	$\langle VFE/V1 \rangle$
CS	10.3	2.3	17.9	30.4	2.3
CSS	15.4	2.4	39.2	27.5	2.05
CSBR	17.05	2.4	50.2	13.3	1.0

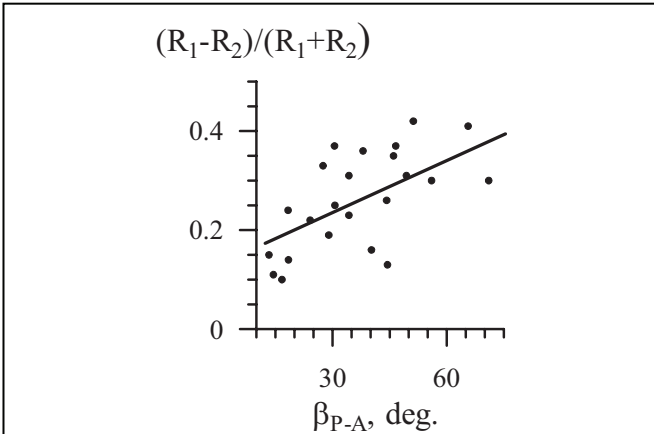


Fig.4. Dependence of the HCME shift relative to the solar disk center along the CME large axis, expressed through the $R = (R_1 - R_2) / (R_1 + R_2)$ parameter, on the β_{P-A} angular position associated with the CMEs of eruptive filaments (post-eruptive arcades). Correlation coefficient is $K = 0.4$.

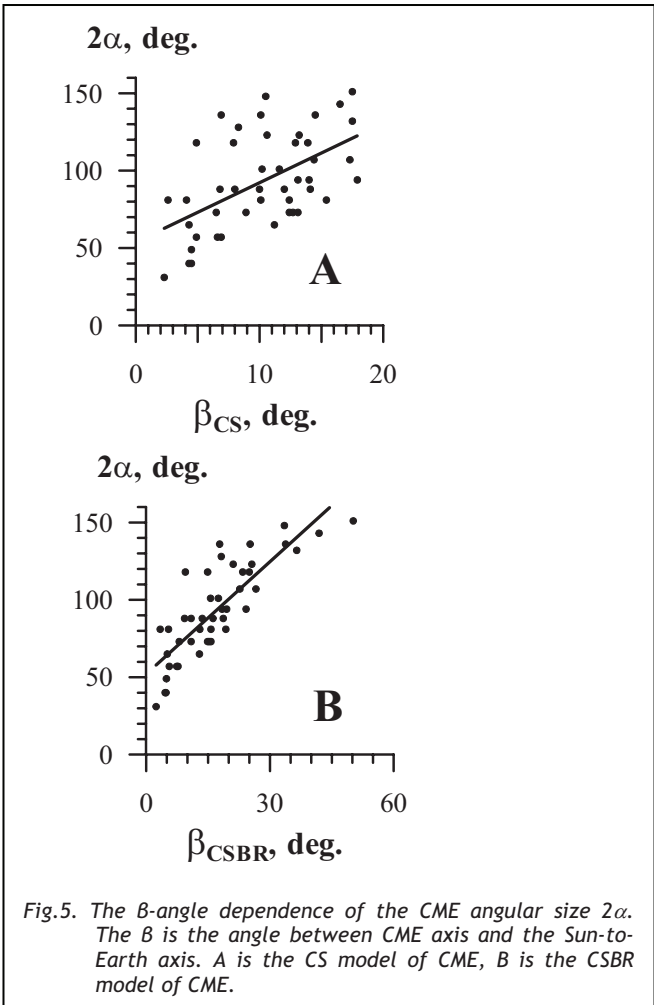


Fig.5. The β -angle dependence of the CME angular size 2α . The β is the angle between CME axis and the Sun-to-Earth axis. A is the CS model of CME, B is the CSBR model of CME.

It has been suggested in [19] that the reason for such a peculiarity in the CME trajectory is the decisive effect on the CME motion at the initial stage produced by the magnetic field in the belt and chains of streamers,

which, as long as CMEs move away from the Sun surface, decline in latitude and longitude from their initial position.

(iii) We showed that the halo CME center shift, expressed by the $\Delta R = (R_1 - R_2)/(R_1 + R_2)$ parameter, relative to the solar disk center along the longer CME axis, depends on the angle position β_{P-A} of the eruptive filament (post-eruptive arcade) associated with the CME, Fig.4.

(iiii) We established that the majority of full halo CMEs under consideration have a relatively large angular size ($2\alpha \sim 30^\circ - 140^\circ$). Thus, the halo CME mean $2\alpha \approx 93^\circ$. This value is essentially larger than the "limb" CME mean angular size $\approx 47^\circ$ [2]. A similar conclusion was made earlier in [13, 15-16].

Fig.5 presents the relationship between the CME halo angular sizes and the CME direction relative to the Sun-to-Earth axis for two CME models: CS and CSBR. One can see that CMEs whose axes most strongly deviate from the Sun-to-Earth axis, have, on average, a larger angular size than CMEs traveling close to the Sun-to-Earth axis. In its turn, the angular difference $\beta - \beta_{P-A}$, on average, increases with increasing β_{P-A} (Fig.6). This means that CMEs whose sources are farther from the Sun-to-Earth axis deviate to that axis at a larger angle.

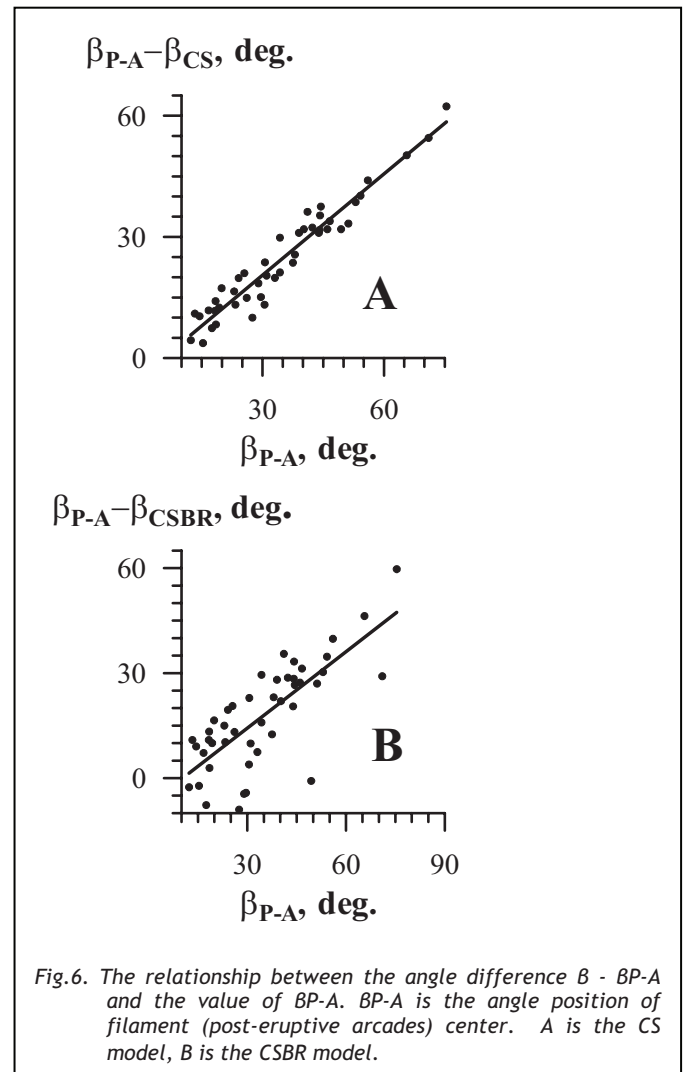


Fig.6. The relationship between the angle difference $\beta - \beta_{P-A}$ and the value of β_{P-A} . β_{P-A} is the angle position of filament (post-eruptive arcades) center. A is the CS model, B is the CSBR model.

Acknowledgements

SOHO is a project of international cooperation between ESA and NASA. This work was supported by RF Leading Scientific Schools Support Governmental Grant SS 4741.2006.2 and by P-16 RAS Presidium Fundamental Research Program.

References

- [1] Howard R.A., Michels D.J., Sheeley N.R. Jr., Koomen M.J., "The observation of a coronal transients directed at Earth" *Astrophys. J.*, 1982, vol. 263, pp. L101-L104.
- [2] Yashiro S., Gopalswamy N., Michalek G., St. Cyr O. C., Plunkett S. P., Rich N. B., Howard R. A. J., "A catalog of white light coronal mass ejections observed by the SOHO spacecraft", *J. Geophys. Res.*, 2004, vol. 109, Issue A7, A07105.
- [3] Webb, D.F., Cliver E.W., Crooker N.U., St. Cyr O.C., Thomson B.J. J., "Relationship of halo coronal mass ejections, magnetic clouds, and magnetic storms", *J. Geophys. Res.*, 2000, vol. 105, pp. 7491-7508.
- [4] Plunkett S.P., Vourlidas A., Simberova S., Karlicky M, Kotrc P., Heinzl P., Kupryakov Yu.A., Guo W.P., Wu S.T., "Simultaneous SOHO and ground-based observations a large eruptive prominence and coronal mass ejection", *Solar Phys.*, 2000, vol. 194, pp. 371-391.
- [5] Zhou C, Wang J., Cao Z., "Correlation between halo coronal mass ejections and solar surface activity", *Astron. & Astrophys.*, 2003, vol.397, pp. 1057-1067.
- [6] Gopalswamy N., Yashiro S., Michalek G., Xie H., Makela P., Vourlidas A., and Howard R. A. "A catalog of halo coronal mass ejections from SOHO", *Sun and Geosphere*, 2010, vol.5(1), pp.7-16.
- [7] Gopalswamy N., Yashiro S., Michalek G., Stenborg G., Vourlidas A., Freeland S. and Howard R. "The SOHO/LASCO CME catalog", *Earth, Moon, and Planets*, 2009, vol. 104, pp. 295-313.
- [8] St. Cyr O.C., Howard R.A., Sheeley N.R., Jr., Plunkett S.P., Michels D.J., Paswaters S.E., Koomen M.J., Simnett G.M., Thomson B.J., Gurman J.B., Schwenn R., Webb D.F., Hildner E., Lamy P.L. J., "Properties of coronal mass ejections: SOHO LASCO observations from January 1996 to June 1998", *J. Geophys. Res.*, 2000, vol. 105, pp. 18,169-18,185.
- [9] Zhao X. P., Plunkett S.P. and Liu W., "Determination of geometrical and kinematical properties of halo coronal mass ejections using the cone model", *J. Geophys. Res.*, 2002, vol. 107, No. A8, 1223, pp. SSH (13-1) - (13-9), 10.1029/2001JA009143.
- [10] Zhao X. P., "Determination of geometrical and kinematical properties of frontside halo coronal mass ejections (CMEs)", in: *Coronal and Stellar Mass Ejections*, Proc. IAU Symposium No. 226, K.P. Dere, J. Wang & Y. Yan, eds, 2005, pp. 42-47.
- [11] Michalek G., Gopalswamy N. and Yashiro S., "A new method for estimating widths, velocities, and source location of halo coronal mass ejections", *Astrophys. J.*, 2003, vol. 584, pp. 472-478.
- [12] Xie H., L. Offman and G. Lawrence, "Cone model for halo CMEs: Application to space weather forecasting", *J. Geophys. Res.*, 2004, vol. 109, A03109, doi:10.1029/2003JA010226.
- [13] Cremades H. and Bothmer V., "On the three-dimensional configuration of coronal mass ejections", in: *Coronal and Stellar Mass Ejections*, Proc. IAU Symposium No. 226, K.P. Dere, J. Wang & Y. Yan, eds, 2005, pp. 48-53.
- [14] Hue X.H., C.B. Wang, and X.K. Dou, "An ice-cream cone model for coronal mass ejections", *J. Geophys. Res.*, 2005, vol. 110, A08103, doi:10.1029/2004A010698.
- [15] Michalek G., "An asymmetric cone model for halo coronal mass ejections", *Solar Phys.*, 2006, vol. 237, pp. 101-118.
- [16] Fainshtein V.G., "Method for determining the parameters of full halo coronal mass ejections", *Geomagnetism and Aeronomy*, 2006, vol. 46, pp. 339-349.
- [17] Fisher R.R. and Munro R.H., "Coronal transient geometry", *Astrophys. J.*, 1984, vol. 280, pp. 428-439.
- [18] Schwenn R., Dal Lago A., Huttunen E. and Gonzales W.D. "The association of coronal mass ejections with their effects near the Earth", *Ann. Geophys.*, 2005, v. 23, pp. 1033-1059.
- [19] Fainshtein V.G., "Some regularities in the relationship of limb coronal mass ejections with eruptive prominences and post-eruptive arcades", *Cosmic Research*, 2007, vol. 45, pp. 384-392.
- [20] Fainshtein V.G., "The expansion of coronal mass ejection in the field of view of SOHO/LASCO: some regularities", Proc. 11th Pulkovo International Conference on Solar Physics, St.-Petersburg, 2007, pp.361-364.
- [21] Gopalswamy, N., Dal Lago,A., Yashiro, S., Akiyama, S. "The expansion and radial speeds of coronal mass ejections", *Central European Astrophysical Bulletin*, 2009, vol. 33, pp. 115-124.
- [22] Michalek, G., Gopalswamy, N., Yashiro, S. "Expansion speed of coronal mass ejections", 2009, *Solar Phys.*, vol. 260, pp.401-406.